# Ru(0001) Model Catalyst under Oxidizing and Reducing Reaction Conditions: In-Situ High-Pressure Surface X-ray Diffraction Study

**ARTICLE** *in* THE JOURNAL OF PHYSICAL CHEMISTRY B · DECEMBER 2005

Impact Factor: 3.3 · DOI: 10.1021/jp0538520 · Source: PubMed



**4 AUTHORS**, INCLUDING:

Yunbin He
Hubei University
**80** PUBLICATIONS **1,191** CITATIONS
SEE PROFILE

Edvin Lundgren
Lund University
**231** PUBLICATIONS **5,793** CITATIONS
SEE PROFILE

Herbert Over
Justus-Liebig-Universität Gießen
**196** PUBLICATIONS **5,898** CITATIONS
SEE PROFILE

# Ru(0001) Model Catalyst under Oxidizing and Reducing Reaction Conditions: In-Situ High-Pressure Surface X-ray Diffraction Study

**Y. B. He,[†] M. Knapp,[†] E. Lundgren,[‡] and H. Over*[,†]**

*Department of Physical Chemistry, Justus-Liebig University, Heinrich-Buff-Ring, D-35392 Giessen, Germany, and Department of Synchrotron Radiation Research, University of Lund, Sölvegetan 14, 22362 Lund, Sweden*

*Received: July 13, 2005; In Final Form: September 14, 2005*

With surface X-ray diffraction (SXRD) using a high-pressure reaction chamber we investigated in-situ the oxidation of the Ru(0001) model catalyst under various reaction conditions, starting from a strongly oxidizing environment to reaction conditions typical for CO oxidation. With a mixture of $O_2$ and CO (stoichiometry, 2:1) the partial pressure of oxygen has to be increased to 20 mbar to form the catalytically active $RuO_2$(110) oxide film, while in pure oxygen environment a pressure of $10^{-5}$ mbar is already sufficient to oxidize the Ru(0001) surface. For preparation temperatures in the range of 550−630 K a self-limiting $RuO_2$(110) film is produced with a thickness of 1.6 nm. The $RuO_2$(110) film grows self-acceleratedly after an induction period. The $RuO_2$ films on Ru(0001) can readily be reduced by $H_2$ and CO exposures at 415 K, without an induction period.

## 1. Introduction

In recent years, significant research has focused on the initial oxidation of metal surfaces by experimental as well as by theoretical techniques.[1−9] This interest is not only spurred by its importance in practical applications such as heterogeneous catalysis, corrosion, protective oxide layers, or insulating layers in microelectronic devices but also because of a lack of information on the fundamental processes that determine the initial oxidation of metal surfaces on the atomic scale. In general, the chemisorption of oxygen precedes the actual oxidation of a metal surface.[10] Only after a critical oxygen coverage has been reached, oxygen penetration including the development of a surface oxide may set in.[6,11] A carefully studied exception from this generally accepted rule is the oxidation of Zr(0001).[12] On a Zr(0001) surface, oxygen dissociates and penetrates right away in the subsurface region.[12] Beyond a critical subsurface O coverage of 1 monolayer, additional oxygen is stabilized on the surface, forming an O−Zr−O trilayer. Similar processes are expected to be relevant for Ta, Ti, and V. In the meanwhile this O−Me−O trilayer motif (Me stands for a metal) has also been identified to play a key role in the initial growth of other metal oxides. Rhodium oxide, for example, forms O−Rh−O trilayers during the initial oxidation of Rh(111).[7] For the oxidation of Ru(0001) it has been argued on the basis of density functional theory (DFT) calculations[13] and supported by recent X-ray photoelectron spectroscopy (XPS) measurements[14,15] that an O−Ru−O trilayer exists as a metastable structure, being a precursor to surface $RuO_2$.

The initial oxidation of Ru(0001) was proposed to proceed in an autocatalytic process.[16] The saturation coverage of chemisorbed oxygen on Ru(0001) is reached with a Ru(0001)−(1 × 1)O surface at 1 monolayer,[17] while the formation of an oxide has been observed only for coverages higher than 3 monolayers.[18] The oxide formation requires large $O_2$ exposures since the sticking coefficient of oxygen on the Ru(0001)−(1 × 1)O surface is of the order of $10^{-6}$.[19] However, as soon as $RuO_2$ nuclei are formed, the further oxidation of Ru(0001) takes place from these nuclei in a self-accelerated process[16,20] since the dissociative sticking coefficient of $O_2$ on $RuO_2$ is as high as 0.8.[19] In other words, the $RuO_2$ nuclei catalyze the oxidation of Ru(0001).

Here we report on "high-pressure" surface X-ray diffraction (SXRD) experiments which allow us to follow in-situ and on atomic scale the oxidation of the model catalyst Ru(0001) under a variety of reaction conditions, such as pure oxygen atmosphere and a mixture of CO and $O_2$ up to 30 mbar at various temperatures. Under these reaction conditions we observed after an induction period a self-limiting growth of $RuO_2$ films which consist of $RuO_2$ domains with a mean size of about 10 nm and a mean thickness of about 5 monolayers. We studied also in-situ the reduction of such prepared $RuO_2$ films on Ru(0001) by $H_2$ and CO exposures.

## 2. Experimental Details

The SXRD experiments were performed at beam line ID03 at the ESRF, using a specially designed ultrahigh-vacuum/high-pressure chamber mounted on a high-precision diffractometer.[21] A photon energy of 17 keV was selected with a Si(111) double monochromator corresponding to a wavelength of 0.73 Å. This experimental setup is truly unique in the in-situ study of structural changes on model catalyst's surfaces under realistic reaction conditions such as those encountered with the initial oxidation of metal surfaces. The cleanliness of the surface is maintained as good as under ultrahigh-vacuum conditions. So far very few in-situ experiments on the initial oxidation of metal surfaces have been reported in the literature[9,22−24] which aim at unraveling microscopic reaction steps under realistic reaction conditions.

The Ru(0001) sample was prepared by Ar-ion etching ($U$ = 2 kV, $I$ = 15 mA, $p$(Ar) = $10^{-5}$ mbar, for 20 min at 760 K) and oxygen treatment cycles at elevated temperatures. The initial

* Corresponding author. Fax: +49-641-99-34559. E-mail: herbert.over@phys.chemie.uni-giessen.de.
[†] Justus-Liebig University.
[‡] University of Lund.

10.1021/jp0538520 CCC: $30.25 
Published on Web 10/22/2005

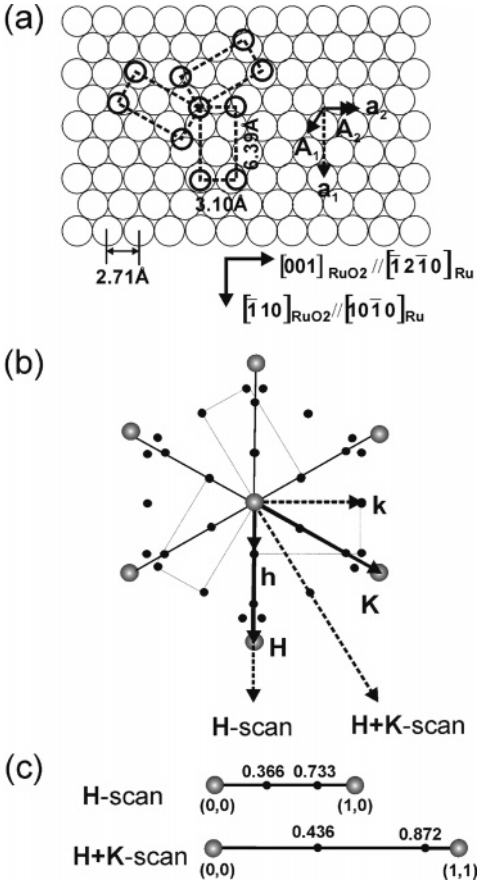


**Figure 1.** (a) Top view of $RuO_2(110)$ grown on Ru(0001). The in-plane lattice vectors $\mathbf{A_1}$ and $\mathbf{A_2}$ and the out-of-plane lattice vector $\mathbf{A_3}$ define the crystal lattices of Ru(0001): $A_1 = A_2 = 2.71$ Å; angle = 120°; $A_3 = 4.28$ Å. The $RuO_2(110)$ surface is oriented along the $\mathbf{A_3}$ axis of Ru(0001). The in-plane lattice vectors of $RuO_2(110)$ are depicted in a, forming a rectangular surface unit cell, defined by the lattice vectors $\mathbf{a_1}$ and $\mathbf{a_2}$. The in-plane epitaxial growth relationship between the $RuO_2(110)$ film and the Ru(0001) substrate is indicated, i.e., $RuO_2$-$[001]//Ru[\bar{1}2\bar{1}0]$ and $RuO_2[\bar{1}10]//Ru[10\bar{1}0]$. In reciprocal space (b), **H** and **K** are the in-plane lattice vectors and **L** is parallel to $\mathbf{A_3}$. The reciprocal lattice vectors of $RuO_2(110)$ are **h**, **k**, **l**, where **h** is parallel to **H** and **k** is aligned along an equivalent direction of **H** + **K**, while **l** and **L** are parallel. (c) Illustration of the **H** and **H** + **K** scans, indicating the positions of expected diffraction maxima of $RuO_2(110)$ with respect to Ru(0001).

oxidation of the Ru(0001) was monitored in situ by SXRD while exposing the sample to various $O_2$ and CO partial pressures (ranging from $10^{-5}$ mbar to some 10 mbar) at sample temperature ranging from 550 to 750 K. Reduction of $RuO_2$ films on Ru(0001) was carried out by $H_2$ or CO exposure at 415 K.

### 3. Results and Discussion

In Figure 1 the lattice vectors of the Ru(0001) surface are shown which define the crystal lattice of the hexagonal close packed (hcp) crystal. In reciprocal space, **H** and **K** are the in-plane lattice vectors corresponding to $\mathbf{A}_1$ and $\mathbf{A}_2$ in Figure 1a, and **L** is the out-of-plane vector. The reciprocal lattice vectors of the tetragonal $RuO_2(110)$ on Ru(0001) are given in fractions of **H**, **K**, and **L**, and are annotated as **h**, **k**, **l**, where **h** is parallel to **H** and **k** is equivalent to the **H** + **K** (by mirror plane symmetry) direction (cf. Figure 1), while **l** is aligned along the **L** direction.

Before presenting the experimental data, we summarize briefly those structural properties of $RuO_2$,[25] which are important for the discussion of our SXRD experiments. $RuO_2$ crystallizes

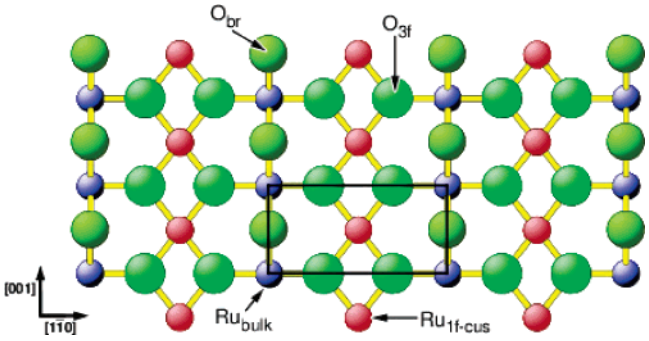


**Figure 2.** Stick and ball model of the stoichiometric $RuO_2(110)$ surface. The small balls (red and blue) are Ru atoms; the large balls represent oxygen atoms. The catalytic activity of the $RuO_2(110)$ surface is determined by the under-coordinated Ru ($Ru_{1f-cus}$, red) and bridging oxygen atoms ($O_{br}$). Bulk Ru atoms are small blue balls. The Ru atoms form in-plane a centered unit cell indicated by the rectangle.

in the rutile structure. On the hexagonal Ru(0001) surface an unstrained $RuO_2$ film (tetragonal structure) grows epitaxially and incommensurately. The flat oxide surface is oriented along the (110) direction, while in-plane three rotational domains (rotated by 120° with each other) coexist for symmetry reasons (*P*2*mm* of $RuO_2$ versus *P*3*m*1 of Ru(0001); cf. Figure 1a,b). The Ru sublattice of $RuO_2(110)$ forms a centered unit cell (see Figure 2). Because Ru is a much stronger X-ray scatterer than O, we expect for a $RuO_2(110)$ film strong intensities only for even diffraction order of **h** + **k**.

The first experiment was designed to study in-situ the oxidation of Ru(0001) in a pure molecular oxygen atmosphere (the background pressure in the high-pressure chamber was $2 \times 10^{-9}$ mbar). With SXRD we measured **H** and **H** + **K** scans (defined in Figure 1c) at $L = 0.2$ as well as the **L** scan at ($H$, $K$) = (0.733, 0), while the Ru(0001) surface was exposed to $10^{-5}$ mbar of molecular oxygen, keeping the sample temperature at 630 and 580 K, respectively (see Figure 3). After an induction period of about 20 min a distinct diffraction peak occurs at 0.733 in the **H** scan (cf. Figure 3a), which corresponds to the second-order diffraction; the peak at 0.3665 is too small to be detectable. After the induction period the X-ray diffraction intensities at $H = 0.733$ increase steeply with exposure time, finally saturating after 60 min. The found induction period together with the steep raise in intensity (see inset of Figure 3a) is reconciled with an autocatalytic oxidation process of Ru(0001). In the **H** + **K** scan additional peaks appear at 0.436 and 0.872 (cf. Figure 3b). The intensity of the 0.436 peak is much smaller than that of the 0.872 peak consistent with the centered surface unit cell of the Ru sublattice of $RuO_2(110)$.

From the in-plane lattice parameters $H = 0.733/2$ and $H = K = 0.436$ in reciprocal space we derive the (real space) in-plane lattice parameters of the $RuO_2$ film to be 3.10 Å × 6.39 Å. These values correspond nicely to the bulk-truncated unit cell of $RuO_2(110)$, namely, 3.11 Å × 6.38 Å as expected for an unstrained $RuO_2(110)$ film on the Ru(0001) surface.

The evolution of the **H** scan does not indicate any variation in the full-width at half-maximum (fwhm). The fwhm of the peak at 0.733 in the **H** scan keeping $L = 0.2$ and 1.3 (not shown) is in both cases 0.018. Therefore the averaged lateral dimension of the $RuO_2$ domains along the $[\bar{1}10]$ direction is approximately 150 Å. The fwhm of the peak at 0.872 in the **H** + **K** scan at $L = 1.3$ is 0.016 which corresponds to a domain size of approximately 80 Å along the [001] direction. Both estimated dimensions are in line with recent scanning tunneling microscopy (STM) images of $RuO_2(110)$ films on Ru(0001).[26,27] In a previous STM study[26] we observed that $RuO_2(110)$ domains

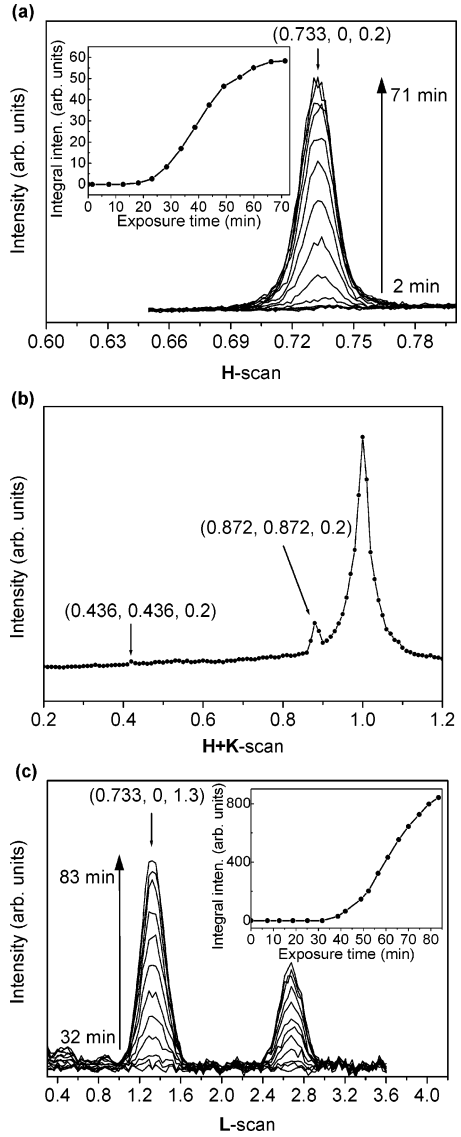


**Figure 3.** Monitor the oxidation of the Ru(0001) sample by in-situ SXRD. (a) Evolution of the **H** scan with exposure time when exposing the Ru(0001) sample to $p(O_2) = 10^{-5}$ mbar at a sample temperature of 630 K. In the inset the integral intensity is shown as a function of oxygen exposure time. The peak at 0.733 is the second-order reflection of $RuO_2(110)$ along the **H** direction. (b) Corresponding **H** + **K** scan of the final $RuO_2$ film. (c) Evolution of **L** scans with exposure time when exposing the Ru(0001) sample to $p(O_2) = 10^{-5}$ mbar at a sample temperature of 580 K. In the inset the integral intensity is displayed as a function of oxygen exposure time.

coexist with $(1 \times 1)$O, covering comparable fractions of the surface. Since $RuO_2(110)$ grows incommensurately on Ru(0001), the intensity of $RuO_2$-related diffraction spots are only affected by the oxide layer but not by the $(1 \times 1)$O phase. In contrast the crystal truncation rods depend strongly on both the $(1 \times 1)$O patches and the $RuO_2(110)$/Ru(0001) interface therefore being difficult to analyze. We thus restrict our current discussion only to $RuO_2$-related diffraction spots.

We also measured the evolution of the **L** scans for $(H, K) = (0.733, 0)$ during the oxidation of Ru(0001) (cf. Figure 3c). **L** scans probe the out-of-plane periodicity of the $RuO_2(110)$ film. The $(H, K) = (0.733, 0)$ diffraction beam is predominantly sensitive to the Ru sublattice of the $RuO_2(110)$ film. After an induction period of about 30 min (cf. Figure 3c) two distinct maxima evolve in the **L** scan, namely, at $L = 1.3$ and at $L = 2.6$. The different induction periods of the **H** (cf. Figure 3a) and **L** scans (cf. Figure 3c) are related to the different sample temperatures (630 K versus 580 K). An increase of the background intensity in the **L** scans upon oxidation is not observed so that the presence of a single well-ordered O−Ru−O trilayer or a single crystalline $RuO_2$ wetting layer cannot be identified with SXRD. From the fwhm of the peaks in the **L** scan we estimate the thickness of the $RuO_2(110)$ to be 1.6 nm; i.e., the $RuO_2$ film consists of five $RuO_2$ layers. The fwhm of the maxima in the **L** scans does not change during the oxidation of Ru(0001). The vertical growth of the $RuO_2(110)$ oxide film is self-limited. From the separation of the maxima in the **L** scan we infer that the Ru subplanes in the $RuO_2(110)$ domain are separated by 3.2 Å, in perfect agreement with the bulk layer spacing of $RuO_2(110)$ structure (3.23 Å[25]).

**TABLE 1: Oxidation of Ru(0001) in Pure Oxygen Environment for Various Preparation Temperatures *T***

| *T*/K | $p(O_2)$/mbar | fwhm(**L**) | no. of $RuO_2$ layers |
|---|---|---|---|
| 580 | $1.3 \times 10^{-5}$, $1.1 \times 10^{-3}$, $1.2 \times 10^{-2}$ | 0.29 | 5.0 |
| 600 | $1.0 \times 10^{-4}$, $2 \times 10^{-3}$, $2 \times 10^{-2}$, $1.0 \times 10^{-1}$ | 0.29 | 5.0 |
| 630 | $5.0 \times 10^{-5}$ | 0.26 | 5.6 |
| 670 | $5.0 \times 10^{-5}$, $1 \times 10^{-1}$ | 0.19 | 7.7 |
| 720 | $5.0 \times 10^{-5}$ | 0.13 | 11.2 |

The fwhm(**L**) are taken for the maximum at $L = 1.3$ in the **L** scan for $H = 0.733$ and $K = 0.0$. From these values we estimate the number of $RuO_2$ layers in the oxide by 1.33/(fwhm(**L**) × 0.91). The correction factor 0.91 was taken from the literature.[36] The separation between the two maxima in the **L** scans is 1.33.

Similar SXRD results were obtained for the oxidation at various preparation temperatures in the range of 580−650 K. The thicknesses and domain sizes of these $RuO_2$ films are compiled in Table 1. Obviously, the thickness of the $RuO_2$ domains is practically constant (5−6 $RuO_2$ layers) in the temperature range of 580−630 K. We varied also the partial pressure of oxygen in the range of $10^{-5}$−$10^{-1}$ mbar. The thickness of the $RuO_2$ film was not affected by the variation of $O_2$ pressure. For sample temperatures of 670 and 720 K the thickness of the $RuO_2$ film increases significantly. However, also a faceting of the $RuO_2$ film took place. The lateral $RuO_2$ domain size does not change when the preparation temperature is varied from 580 to 720 K.

If the preparation temperature was chosen to be lower than 540 K (even for an $O_2$ pressure of $10^{-1}$ mbar), the Ru(0001) surface did not form a crystalline oxide film. This result is consistent with recent scanning photoelectron microscopy (SPEM) investigations.[15] Here it is important to recall that SXRD is only sensitive to those parts of the surface which are well-ordered. This means that SXRD is "blind" to amorphous or weakly ordered structures such as $Ru_xO_y$ which was recently proposed by a XPS study.[14]

The most intriguing feature of these SXRD measurements is that the fwhm of $RuO_2$-related diffraction peaks does not vary during the oxidation process, neither in-plane (**H**, **H** + **K** scan) nor out-of-plane (**L** scan). We have to recall that the transfer width of the incident X-ray beam is several micrometers. Rocking scans around the surface normal from the Ru(0001) crystal surface at the minimum of a crystal truncation rod indicates an averaged terrace width of Ru(0001) of 500 nm. Therefore, the observed fwhm values are solely determined by the $RuO_2$ domain size which is around 10 nm across and 1.6 nm in thickness. The observed increase of the X-ray diffraction intensities of $RuO_2$-related diffraction spots in the **H**, **H**+**K** and **L** scans upon $O_2$ exposure is, therefore, associated with a growing number of such $RuO_2$ domains whose diffraction

intensity contributes incoherently to the measured diffraction intensity. To ensure that the diffraction intensity of each $RuO_2$ domain sums up incoherently, the $RuO_2$ domain must not be in registry with respect to the in-plane $RuO_2(110)$ lattice; otherwise the fwhm of the maxima in the **H** and **H** + **K** scans would decrease with an increase of the $O_2$ exposure time. Since the $RuO_2(110)$ domains grow incommensurately on the substrate Ru(0001) surface, they are incoherent to each other, thus contributing additively to diffraction intensity. We note that the growth of a single $RuO_2$ domain cannot be time-resolved by the present SXRD experiment with its time resolution of about 100 s.

The time evolution of $RuO_2$-related diffraction intensities during oxygen exposure discloses an induction period (cf. Figure 3) which can be explained by the time required to form the first $RuO_2$ domains on the Ru(0001) surface. The further lateral growth of the $RuO_2(110)$ film is then promoted by these already existing $RuO_2(110)$ domains in that new $RuO_2$ domains preferentially form in their vicinity. Consequently, the oxide growth becomes self-accelerated. Accordingly, the $RuO_2(110)$ film consists of $RuO_2(110)$ domains which bunch together consistent with recent STM images, indicating a flakelike pattern of the $RuO_2(110)$ film.[26]

For the reduction experiments we produced first a 1.6 nm thick $RuO_2(110)$ film on Ru(0001), consisting of $RuO_2$ domains with dimensions of about 10 nm across. This oxide film was subsequently reduced by hydrogen exposure of $p(H_2) = 10^{-5}$ mbar, keeping the sample temperature at 417 K. The progressing reduction of $RuO_2$ by $H_2$ was monitored in-situ by both the evolution of the **L** scan and that of the **H** scan (cf. Figure 4). The integral X-ray intensities of the $H = K = 0.872$ and $L = 1.3$ peak are shown in the insets of Figure 4a,b as a function of the $H_2$ exposure time. No induction period occurred within the experimental time resolution of 100 s. The integral intensity of this peak decreases linearly with $H_2$ exposure time. The fwhm of the peaks in the **L** and **H** + **K** scans does not change with $H_2$ exposure time, indicating that neither the averaged size nor the thickness of the $RuO_2$ domains varies during the reduction process by $H_2$ exposure. The reduction of the $RuO_2(110)$ film thus appears to proceed via the annihilation of complete $RuO_2$ domains. Since no induction period is observed, the $H_2$ reduction of $RuO_2(110)$ film differs from the reduction of $Rh_2O_3$ for which an autocatalytic process was identified.[28] For lower temperatures we have not observed any reduction of the $RuO_2$ film by hydrogen exposure. The threshold temperature, where the reduction by hydrogen exposure sets in, is around 400 K, consistent with recent $H_2$ oxidation experiments.[29]

Similar reduction experiments were performed by dosing CO. The thickness of the starting $RuO_2$ film was 1.6 nm; the lateral domain size was 10 nm. Upon CO exposure ($p(CO) = 10^{-5}$ mbar) at a sample temperature of 415 K, the integral intensity of the $H = 0.733$ peak at $K = 0$ and $L = 0.5$ decreased linearly with time (cf. Figure 4c). Again neither the fwhm of the **H** scans nor that of the **L** scans changed, indicating a reduction process similar to that for hydrogen.

In a subsequent experiment we oxidized the Ru(0001) surface by a mixture of CO and $O_2$ (CO:$O_2$ stoichiometry, 1:2). The scientific background to this experiment is that we had not been able to produce an oxide under ultrahigh-vacuum condition as soon as we used a gas mixture of CO and $O_2$.[30] However, supported and unsupported Ru catalysts oxidize readily under oxidizing reaction conditions, where CO and $O_2$ are both present in the gas feed.[31,32] Another motivation for this experiment is to understand the CO oxidation experiments by Peden and Goodman.[33] Peden and Goodman showed that under ultrahigh-vacuum conditions Ru(0001) is inactive in the oxidation of CO. However, under higher pressures in the millibar range, Ru(0001) turned into a very active oxidation catalyst, whose active phase has not been identified unequivocally.

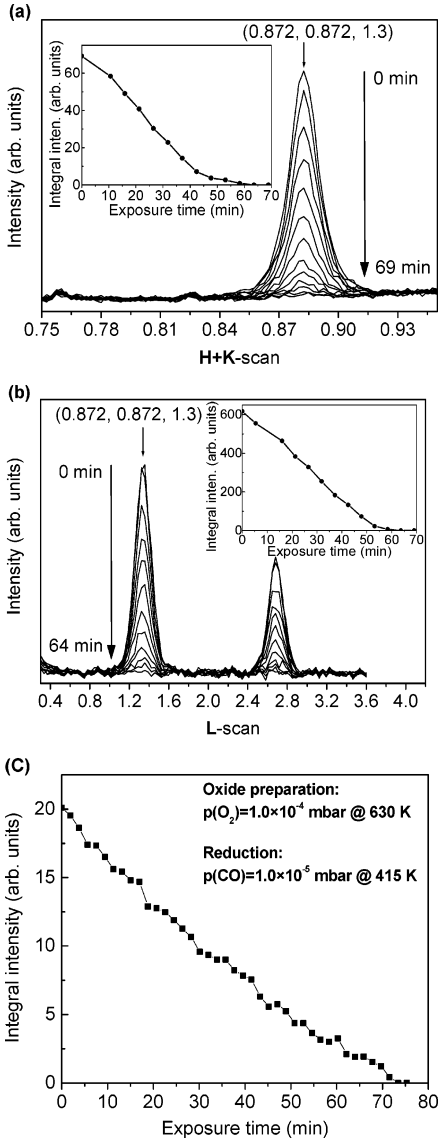


**Figure 4.** Reduction of a 5 monolayer thick $RuO_2(110)$ film grown on Ru(0001) by exposure to $10^{-5}$ mbar of $H_2$ at a sample temperature of 417 K. (a) Evolution of **H** + **K** scans depending on the exposure time. In the inset the integral intensities are shown as a function of $H_2$ exposure time. (b) Evolution of **L** scan depending on the exposure time. In the inset the integral intensities are indicated as a function of $H_2$ exposure time. (c) Reduction of a 5 monolayer thick $RuO_2(110)$ film on Ru(0001) by exposure to $10^{-5}$ mbar of CO at a sample temperature of 415 K. The integral intensities of the peak at 0.733 along the **H** direction are depicted as a function of exposure time.

With a mixture of CO and $O_2$ of up to 10 mbar in total pressure no oxidation of the Ru(0001) was observed with in-situ SXRD and within 2000 s, keeping the sample temperature at 630 K. However, if we increased the total CO + $O_2$ pressure to 28 mbar, then after an induction period of 700 s the oxidation of Ru(0001) set in spontaneously and was completed within one single **H** scan (i.e. within 100 s; cf. Figure 5a,b). In comparison to the oxidation at $10^{-5}$ mbar of pure oxygen, the complete surface oxidation of Ru(0001) by 28 mbar of CO + $O_2$ proceeds much faster, indicating that kinetic hindrance was the main reason for the retarded oxidation of Ru(0001) by a

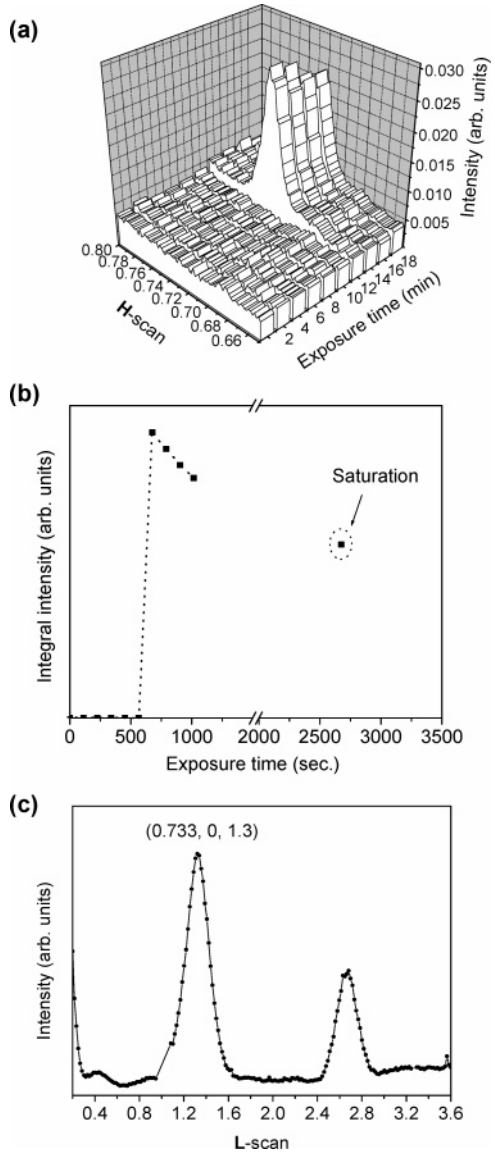


**Figure 5.** Oxidation of the Ru(0001) sample by exposing it to a gas mixture of $O_2$ and CO: $p(O_2) = 18$ mbar and $p(CO) = 10$ mbar at a sample temperature 630 K. (a) Evolution of the **H** scan with exposure time. (b) Integral intensity as a function of exposure time. (c) **L** scan for the final $RuO_2(110)$ film. From the separation between the two peaks at $L = 1.3$ and 2.6 a layer distance of 3.2 Å is inferred, while the fwhm of these peaks indicates a $RuO_2$ film thickness of 1.6 nm.

1:2 CO + $O_2$ gas mixture. From the fwhm of the **H** scan and **H** + **K** scan we estimate the averaged $RuO_2$ domain size again to be 10 nm across. From the fwhm of the **L** scan the averaged thickness of the $RuO_2(110)$ domains is derived to be 1.6 nm. The $RuO_2(110)$ film is very flat as indicated by the small modulations between the Bragg reflection in the **L** scans (cf. Figure 5c).

The long induction period together with the high CO + $O_2$ pressure of 28 mbar required to oxidize the Ru(0001) sample suggests that the oxidation of the first $RuO_2$ domain imposes the rate-determining step. Several scenarios are conceivable. Either we need a large critical size of a $RuO_2$ nucleus to initiate the oxidation of the first $RuO_2$ domain. The formation of such a $RuO_2$ nucleus is subject to reduction by CO so that the critical size of the nucleus is only stable when the pressure of oxygen is high enough. Or an alternative scenario, which we do not favor, is that the nucleation of $RuO_2$ domains needs a critical mass of incorporated oxygen. Once it is reached the growth of $RuO_2(110)$ proceeds rather fast for thermodynamical reasons.[34] In any case the oxide growth is self-accelerated and spreads across the Ru(0001) surface. From Figure 5b it is evident that when the complete $RuO_2$ film has formed, further CO + $O_2$ exposure leads even to a partial decrease of the integral intensity of the $H = 0.733$ peak. We may speculate that this decrease is related to a partial roughening of the $RuO_2$ film. Finally, for exposure times longer than 3000 s the $RuO_2$ film is stable; i.e., the model catalyst has reached steady-state conditions.

These CO + $O_2$ experiments clearly show that $RuO_2(110)$ is the active phase in the high-pressure CO oxidation experiments over Ru(0001) of Peden and Goodman.[33] The CO + $O_2$ experiment confirms also nicely the *core shell model* of Assmann et al., which was proposed for supported[31] and powder[32,35] Ru catalysts. For these practical Ru-based catalysts an ultrathin (self-limiting) $RuO_2$ film of about 1−2 nm was postulated to cover the Ru metal core of the Ru particles in order to explain the in-situ reaction experiments and the in-situ Fourier Transform Infrared (FTIR) experiments in combination with the hydrogen reduction experiments.[31,32,35] Here with the Ru(0001) surface, serving as the corresponding model catalyst, we identify also a kind of core shell model in which the Ru(0001) surface is covered by a self-limiting grown $RuO_2(110)$ film whose thickness is 1.6 nm.

## 4. Conclusion

With surface X-ray diffraction experiments using a dedicated high-pressure reaction chamber we explored the oxidation of the Ru(0001) model catalyst under reaction conditions which are far beyond the ultrahigh-vacuum regime. In particular, we investigated in-situ the oxidation of the Ru(0001) model catalyst surface under various reaction conditions starting from a strongly oxidizing environment to reaction conditions typical for CO oxidation. With a mixture of $O_2$ and CO (stoichiometry CO:$O_2$ = 1:2) the partial pressure of oxygen has to be increased to 20 mbar in order to form the catalytically active $RuO_2(110)$ oxide film, while with pure oxygen exposure a pressure of $10^{-5}$ mbar is sufficient to oxidize the Ru(0001) surface. In all oxidation experiments a self-limiting surface oxide is produced after an induction period. The $RuO_2$ film consists of $RuO_2(110)$ domains with mean lateral dimensions of 10 nm across. For preparation temperatures in the range of 550−630 K the $RuO_2(110)$ film reveals a thickness of 1.6 nm. The chemical reduction of such ultrathin and flat $RuO_2$ films on Ru(0001) by hydrogen or CO exposure (sample temperature, 415 K) proceeds without an induction period.

**Acknowledgment.** We acknowledge partial financial support from the European Union under Contract No. NMP3-CT-2003-505670 (NANO2) and from the German priority program (SPP1091: Ov21/4). E.L. acknowledges financial support from the Swedish Research Council. We thank Dr. Hyojung Kim from the ID3 beam line staff at ESRF for her skillful technical assistance during the measurements.

## References and Notes

(1) (a) Wilhelmi, G. A.; Brodde, A.; Badt, D.; Wengelnik, H.; Neddermeyer, H. In *The Structure of Surfaces III*; Tong, S. Y., Van Hove, M. A., Xie X. D., Eds.; Springer: Berlin, 1991; p 448. (b) Bertrams, T.; Brodde, A.; Hannemann, H.; Ventrice, C. A.; Wilhelmi, G.; Neddermeyer, H. *Appl. Surf. Sci.* **1994**, *75*, 125.

(2) Liu, W.; Wong, K. C.; Zeng, H. C.; Mitchell, K. A. R. *Prog. Surf. Sci.* **1995**, *50*, 247.

(3) Carlisle, C. I.; King, D. A.; Bocquet, M. L.; Gerda, J.; Sautet, P. *Phys. Rev. Lett.* **2000**, *84*, 3899.

(4) Surnev, S.; Kresse, G.; Ramsey, M. G.; Netzer, F. P. *Phys. Rev. Lett.* **2001**, *87*, 086102.

(5) Lundgren, E.; Kresse, G.; Klein, C.; Borg, M.; Andersen, J. N.; De Santis, M.; Gauthier, Y.; Konvicka, C.; Schmid, M.; Varga, P. *Phys. Rev. Lett.* **2002**, *88*, 246103.

(6) Todorova, M.; Li, W. X.; Ganduglia-Pirovano, M. V.; Stampfl, C.; Reuter, K.; Scheffler, M. *Phys. Rev. Lett.* **2002**, *89*, 096103.

(7) Gustafson, J.; Mikkelsen, A.; Borg, M.; Lundgren, E.; Köhler, L.; Kresse, G.; Schmid, M.; Varga, P.; Yuhara, J.; Torrelles, X.; Quiros, C.; Andersen, J. N. *Phys. Rev. Lett.* **2004**, *92*, 126102.

(8) Li, W. X.; Österlund, L.; Vestergaard, E. K.; Vang, R. T.; Matthiesen, J.; Pedersen, T. M.; Lægsgard, E.; Hammer, B.; Besenbacher, F. *Phys. Rev. Lett.* **2004**, *93*, 146104.

(9) Lundgren, E.; Gustafson, J.; Mikkelsen, A.; Andersen, J. N.; Stierle, A.; Dosch, H.; Todorova, M.; Rogal, J.; Reuter, K.; Scheffler, M. *Phys. Rev. Lett.* **2004**, *92*, 046101.

(10) Over, H. *Prog. Surf. Sci.* **1998**, *58*, 249, and references therein.

(11) Over, H. In *Landolt Börnstein*, Vol 42, Subvolume A, Part 4; Bonzel, H. P., Ed.; Springer-Verlag: Berlin, Heidelberg, Germany, 2005; pp 2−73.

(12) Wang, Y. M.; Li, S.; Mitchell, K. A. R. *Surf. Sci.* **1997**, *380*, 540.

(13) Reuter, K.; Ganduglia-Pirovano, M. V.; Stampfl, C.; Scheffler, M. *Phys. Rev. B* **2002**, *65*, 165403.

(14) Böttcher, A.; Starke, U.; Conrad, H.; Blume, R.; Niehus, H.; Gregoratti, L.; Kaulich, B.; Barinov, A.; Kiskinova, M. *J. Chem. Phys.* **2002**, *117*, 8104.

(15) Blume, R.; Niehus, H.; Conrad, H.; Böttcher, A.; Aballe, L.; Gregoriatti, L.; Barinov, A.; Kiskinova, M. *J. Phys. Chem. B* **2005**, *109*, 14052.

(16) Over, H.; Seitsonen, A. P. *Science* **2002**, *297*, 2003.

(17) Stampfl, C.; Schwegmann, S.; Over, H.; Scheffler, M.; Ertl, G. *Phys. Rev. Lett.* **1996**, *77*, 3371.

(18) Böttcher, A.; Niehus, H.; Schwegmann, S.; Over, H.; Ertl, G. *J. Phys. Chem. B* **1997**, *101*, 11185.

(19) Böttcher, A.; Niehus, H. *Phys. Rev. B* **1999**, *60*, 14396.

(20) Thürmer, K.; Williams, E.; Reutt-Robbey, J. *Science* **2002**, *297*, 2033.

(21) Bernard, P.; Peters, K. F.; Alvarez, J.; Ferrer, S. *Rev. Sci. Instrum.* **1999**, *70*, 1478.

(22) Stierle, A.; Kasper, N.; Dosch, H.; Lundgren, E.; Gustafson, J.; Mikkelsen, A.; Andersen, J. N. *J. Chem. Phys.* **2005**, *122*, 044706.

(23) Stierle, A. *Z. Metallk.* **2002**, *93*, 833.

(24) Hendriksen, B. L. M.; Frenken, J. W. M. *Phys. Rev. Lett.* **2002**, 89, 046101.

(25) Kim, Y. D.; Seitsonen, A. P.; Over, H. *Surf. Sci.* **2000**, *465*, 1.

(26) Over, H.; Kim, Y. D.; Seitsonen, A. P.; Wendt, S.; Lundgren, E.; Schmid, M.; Varga, P.; Morgante, A.; Ertl, G. *Science* **2000**, *287*, 1474.

(27) Over, H.; Seitsonen, A. P.; Lundgren, E.; Schmid, M.; Varga, P. *Surf. Sci.* **2002**, *515*, 143−156.

(28) Dudin, P.; Barinov, A.; Gregoratti, L.; Kiskinova, M.; Esch, F.; Dri, C.; Africh, C.; Comelli, G. *J. Phys. Chem.* **2005**, *109*, 13649.

(29) Knapp, M.; Crihan, D.; Seitsonen, A. P.; Over, H. *J Am. Chem. Soc.* **2005**, *127*, 3236.

(30) Knapp, M.; Crihan, D.; Over, H. Unpublished experiments.

(31) Assmann, J.; Narkhede, V.; Löffler, E.; Hindrichsen, O.; Over, H.; Muhler, M. *J. Phys. Chem.* **2004**, *108*, 14634.

(32) Assmann, J.; Crihan, D.; Knapp, M.; Lundgren, E.; Löffler, E.; Muhler, M.; Narkhede, V.; Over, H.; Schmid, M.; Varga, P. *Angew. Chem., Int. Ed.* **2005**, *116*, 939.

(33) Peden, C. H. F.; Goodman, D. W. *J. Phys. Chem.* **1986**, *90*, 1360.

(34) Stampfl, C. *Catal. Today* **2005**, *105*, 17, and references therein.

(35) Narkhede, V.; Assmann, J.; Muhler; M. *Z. Phys. Chem. (Muenchen)* **2005**, *219*, 975−995.

(36) *Handbook of Surface Science*, Vol. 1: Physical Structure; Unertl, W. N., Ed.; Elsevier: Amsterdam, 1996.